MICROBIOLOGY

Dihydrothiazolo ring-fused 2-pyridone antimicrobial compounds treat *Streptococcus pyogenes* skin and soft tissue infection

Zongsen Zou[1], Pardeep Singh[2], Jerome S. Pinkner[1], Chloe L. P. Obernuefemann[1], Wei Xu[1], Taylor M. Nye[1], Karen W. Dodson[1], Fredrik Almqvist[2]*, Scott J. Hultgren[1]*, Michael G. Caparon[1]*

We have developed GmPcides from a peptidomimetic dihydrothiazolo ring-fused 2-pyridone scaffold that has antimicrobial activities against a broad spectrum of Gram-positive pathogens. Here, we examine the treatment efficacy of GmPcides using skin and soft tissue infection (SSTI) and biofilm formation models by *Streptococcus pyogenes*. Screening our compound library for minimal inhibitory (MIC) and minimal bactericidal (MBC) concentrations identified GmPcide PS757 as highly active against *S. pyogenes*. Treatment of *S. pyogenes* biofilm with PS757 revealed robust efficacy against all phases of biofilm formation by preventing initial biofilm development, ceasing biofilm maturation and eradicating mature biofilm. In a murine model of *S. pyogenes* SSTI, subcutaneous delivery of PS757 resulted in reduced levels of tissue damage, decreased bacterial burdens, and accelerated rates of wound healing, which were associated with down-regulation of key virulence factors, including M protein and the SpeB cysteine protease. These data demonstrate that GmPcides show considerable promise for treating *S. pyogenes* infections.

INTRODUCTION

The emergence of antibiotic resistance threatens health care and agriculture systems worldwide and raises the prospect of a post-antibiotic era. Several factors, including the overuse and misuse of antibiotics, and exposure to environmental reservoirs of antibiotic-resistant bacteria have contributed to rising rates of antibiotic resistance (*1*, *2*). A slowdown in antimicrobial drug development has resulted in reliance on existing antimicrobials, which, when combined with poor antibiotic stewardship, has further exacerbated the development of resistance (*3*, *4*). Thus, there is an urgent need to develop antibiotics that are recalcitrant to resistance development to combat multidrug-resistant pathogens.

Toward this goal, we have developed GmPcides, a new class of synthetic compounds based on a peptidomimetic dihydrothiazolo ring-fused 2-pyridone scaffold. Rational alteration at positions C-2, C-7, and C-8 of the central fragment via various synthetic methodologies has resulted in the development of GmPcides with enhanced antibacterial and drug-like activities (*5*). Among these is GmPcide PS757 with robust bacteriostatic and bactericidal activities against a broad range of multidrug-resistant Gram-positive pathogens (*5*), including vancomycin-resistant *Enterococcus faecalis*, methicillin-resistant *Staphylococcus aureus*, multidrug-resistant *Streptococcus pneumoniae*, clindamycin-resistant *Streptococcus agalactiae*, and erythromycin-resistant *S. pyogenes*, all of which are classified as serious or concerning threats by the Centers for Disease Control and Prevention (*6*). Given the broad-spectrum antibacterial activities of GmPcides against Gram-positive pathogens, the next phase of development is to assess their efficacy for treatment using well-characterized models of Gram-positive infection and biofilm formation.

For this study, we have focused on *S. pyogenes*, a Gram-positive pathogen responsible for more than 500,000 deaths per year, a global burden that approaches that of rotavirus and measles (*7*). In humans, *S. pyogenes* can cause a wide range of diseases, ranging from mild to severe, including pharyngitis (strep throat), scarlet fever, toxic shock syndrome, acute glomerulonephritis, and rheumatic fever (*8*–*11*). Of particular concern are skin and soft tissue infections (SSTIs) that range from superficial infection of the epidermis such as impetigo to severe invasive infections of the dermis and deeper tissues including cellulitis and necrotizing fasciitis (the "flesh-eating disease") (*12*). Despite its sensitivity to many different antibiotics, including β-lactams, the treatment of *S. pyogenes* invasive infection is complicated by factors that include its ability to form biofilm and its ability to secrete a myriad number of toxins. Biofilm is an adherent and structured community of bacteria growing within an extracellular polymeric substance that enhances the community's ability to resist killing by antibiotics (*13*–*15*). Toxins produced by *S. pyogenes* play a major role in damaging host tissue and include several membrane-disruptive hemolysins, immuno-modulating superantigens, plasminogen activators, host cell adhesins, complement-modulating proteins, specific and nonspecific proteases, and multiple other degradative enzymes. Because tissue damage affects the efficiency of antibiotics to kill *S. pyogenes*, treatment strategies for necrotizing disease often include an antibiotic that inhibits expression of tissue-damaging toxins in combination with an antibiotic that targets bacterial growth. The latter typically includes a β-lactam (e.g., piperacillin/tazobactam), while the former includes clindamycin (*12*, *16*, *17*), which at sublethal concentrations in vitro inhibits the expression of several tissue-damaging toxins. However, the use of clindamycin is now threatened by increasing rates of resistance in health care settings (*16*–*18*).

In the present study, we extensively characterized the therapeutic properties of GmPcide PS757 using well-characterized biofilm and murine SSTI models of *S. pyogenes* infection. Our results demonstrate that PS757 was effective against all stages of bacterial growth and biofilm formation in vitro and improved treatment outcomes in a murine SSTI model by decreasing bacterial burdens, reducing levels of tissue damage, attenuating inflammation, and accelerating the rate of wound healing. The sublethal exposure to GmPcides reduced

[1]Department of Molecular Microbiology, Center for Women's Infectious Disease Research, Washington University School of Medicine, St. Louis, MO 63110, USA. [2]Department of Chemistry, Umeå University, SE-90187 Umeå, Sweden.
*Corresponding author. Email: fredrik.almqvist@umu.se (F.A.); hultgren@wustl.edu (S.J.H.); caparon@wustl.edu (M.G.C.)

virulence factor expression, including the expression of two major virulence factors, the surface associated M protein and the secreted SpeB cysteine protease. Together, these results suggest that GmPcides have considerable promise for preventing and treating *S. pyogenes* infections.

RESULTS

GmPcide PS757 is active against both nondividing and dividing streptococcal cells

In our previous study, we have identified a GmPcide PS757 with robust antimicrobial activity against a wide range of multidrug-resistant Gram-positive pathogens, including the *S. pyogenes* that was investigated in the present study (*5*). The minimum inhibitory concentration (MIC) of 0.78 µM PS757 against *S. pyogenes* HSC5 strain as determined in the previous study (*5*) demonstrates its robust bacteriostatic activity. In the present work, we further determined its minimum bactericidal concentration (MBC) against streptococcal cells as 1.56 µM, revealing its effective bactericidal activity as well (Table 1). MIC and MBC concentrations of four types of standard-of-care antibiotics—including penicillin, cefotaxime, vancomycin, and azithromycin against *S. pyogenes* HSC5—were also measured (table S1) and compared with PS757, with the results indicating comparable bacteriostatic and bactericidal activities for PS757 and approved antibiotics. Antimicrobial synergy of PS757 with these four antibiotics was examined using checkerboard method and E test. Despite indifferences were observed for these four pairs of combined antimicrobial treatments, three compounds—including PS757, penicillin, and cefotaxime—were found with two- to fourfold MIC reduction in the combination (table S2), suggesting the prospect of antimicrobial synergy that future investigations should be directed at in the continuing process of GmPcides development. Moreover, in our previous study of GmPcide activity against *E. faecalis,* we find that GmPcides could effectively kill stationary phase nondividing cells and have bacteriostatic activity for cells undergoing division in exponential phase (*5*). In contrast, here, we found that GmPcides were bactericidal against both exponential and stationary phases *S. pyogenes*, with reductions in colony-forming units (CFU) of >6 logs and >5 logs, respectively (Table 1 and fig. S1). Together, these results demonstrate the robust antimicrobial activities of GmPcide PS757 against *S. pyogenes*.

GmPcide PS757 induces nucleoid and cell wall abnormalities

A sublethal concentration of PS757 was determined on the basis of both growth curves [optical density at 600 (OD_{600})] and growth yields (CFU) as 0.4 µM (fig. S2). The examination of PS757-treated cells by transmission electron microscopy (TEM) revealed that when compared to vehicle-treated [dimethyl sulfoxide (DMSO)] cells, challenge with a sublethal concentration (0.4 µM) and with a bactericidal concentration (20 µM), both induced extensive nucleoid abnormalities characterized by a condensed and filamentous nucleoid structure (Fig. 1A). Consistently, previous studies found

Table 1. Antimicrobial activity (µM) of GmPcide PS757 against *S. pyogenes* HSC5.

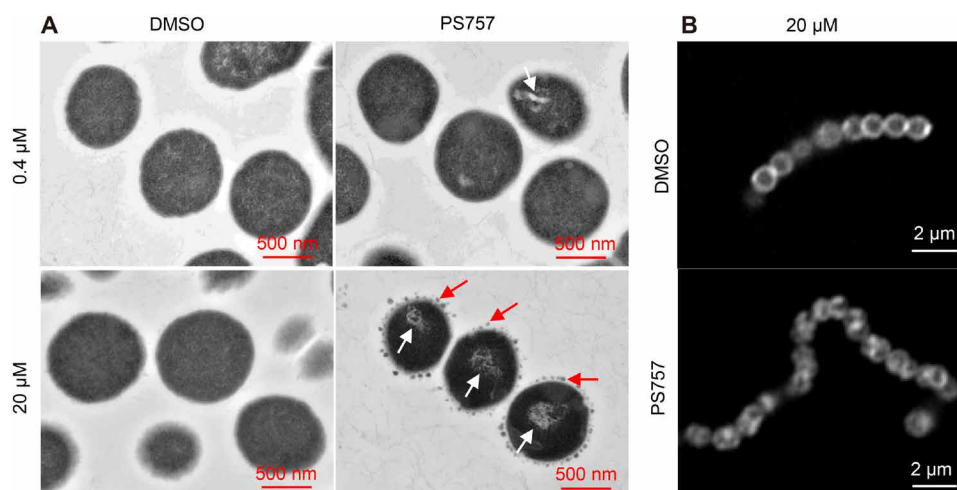| Strain	PS757 (µM)		PS757 (20 µM)	
	MIC	MBC	Exponential	Stationary
S. pyogenes HSC5	0.78*	1.56	>6 logCFU reduction	>5 logCFU reduction

*(*5*).

Fig. 1. GmPcide PS757 treatment caused nucleoid and cell wall abnormalities in *S. pyogenes* cells. (**A**) *S. pyogenes* HSC5 cells treated under both sublethal (0.4 µM) and bactericidal (20 µM) concentrations of PS757 exhibited nucleoid abnormality with altered nucleoid structure that was less dense and very filamentous (white arrows). *S. pyogenes* HSC5 cells treated under bactericidal (20 µM) concentration of PS757 were observed with small dense globular structures at periphery of bacterial cell wall (red arrows), suggesting that PS757 produced cell wall abnormalities. (**B**) *S. pyogenes* HSC5 cells treated under bactericidal (20 µM) concentration of PS757 were observed with irregular and heterogeneous cell wall structures, indicating that PS757 induced cell wall damages. DMSO, dimethyl sulfoxide.

that *Staphylococcus aureus* cells under the treatment of different antimicrobial compounds, e.g., nisin (*19*) and gramicidin S (*20*), were observed with similar DNA damage featuring condensed, fragmented, and inhomogeneous structures, which may result in impeded chromosome replication and segregation (*19, 20*). In addition, streptococcal cells treated at the bactericidal concentration (20 μM) displayed numerous small dense globular structures formed at the periphery of the cell wall (Fig. 1A), similar to the observation of blisters and bubbles appearing in the cell envelopes of *Escherichia coli* cells under the treatment antimicrobial peptide gramicidin S in previous publication (*20*). Moreover, Nile Red–stained streptococcal cells were observed with irregular and heterogeneous cell membrane structures in comparison with the vehicle-treated (DMSO) group (Fig. 1B), suggesting PS757-induced membrane disruption. In summary, our results together with previous findings demonstrate that PS757 may be able to induce nucleoid and cell envelope abnormalities to streptococcal cells, which potentially contribute to its antimicrobial efficacy. Future studies can be directed at investigating the molecular mechanism of PS757, leading to these cell integrity disruptions.

GmPcide PS757 prevents *S. pyogenes* biofilm formation

We used an established model for *S. pyogenes* biofilm formation with brain heart infusion medium (BHI) medium in a 96-well plate format to analyze the efficacy of GmPcides against biofilm. Planktonic growth was measured by OD_{600} (Fig. 2A) and biofilm formation determined using a standard crystal violet (CV) staining assay (Fig. 2B) for cultures in 96-well microplates. In the absence of GmPcide treatment, detectable biofilm began to accumulate at 4 hours after inoculation and continued to develop until reaching maturity at approximately 12 hours (Fig. 2B). *S. pyogenes* biofilm formation was also examined in a culture dish assay characterized by fluorescent confocal microscopy, which showed that a dense biofilm of approximately 9.5 μm in thickness developed at 24 hours after inoculation (fig. S3). To examine the antibiofilm activity of PS757, cultures were then treated at 4, 7, and 24 hours after inoculation (fig. S4, A to C) with a series of different concentrations of PS757 to examine its activity against different phases of biofilm formation. During the initiation phase (4 hours), PS757 at 0.7 and 1.0 μM was able to prevent both planktonic growth and biofilm formation (Fig. 2C). When added to developing biofilm at 7 hours, 2.0 μM PS757 prevented further planktonic growth and at 5.0 μM arrested further maturation of biofilm (Fig. 2D). Last, when used to treat a fully mature biofilm at 24 hours, a concentration of 20 μM produced >90% decrease in cell viability when measured using a fluorescent vital stain and confocal microscopy after 5 hours of treatment (Fig. 2E). In summary, PS757 was efficacious against all phases of *S. pyogenes* biofilm development including initiation and maturation and had the ability to kill cells in a fully mature biofilm.

GmPcide PS757 ameliorates tissue damage in a murine model of SSTI

The well-characterized murine subcutaneous ulcer model of *S. pyogenes* SSTI was used to evaluate the ability of GmPcide PS757 to treat an active infection. In the acute phase of this model, subcutaneous injection of 10^7 CFU of *S. pyogenes* HSC5 into the flanks of 7-week-old SKH1 hairless mice results in a draining ulcer apparent by 24-hour post-infection (PI) with peak bacterial burdens, measured as recovered CFU, obtained at around day 3 PI. To assess the efficacy of GmPcide
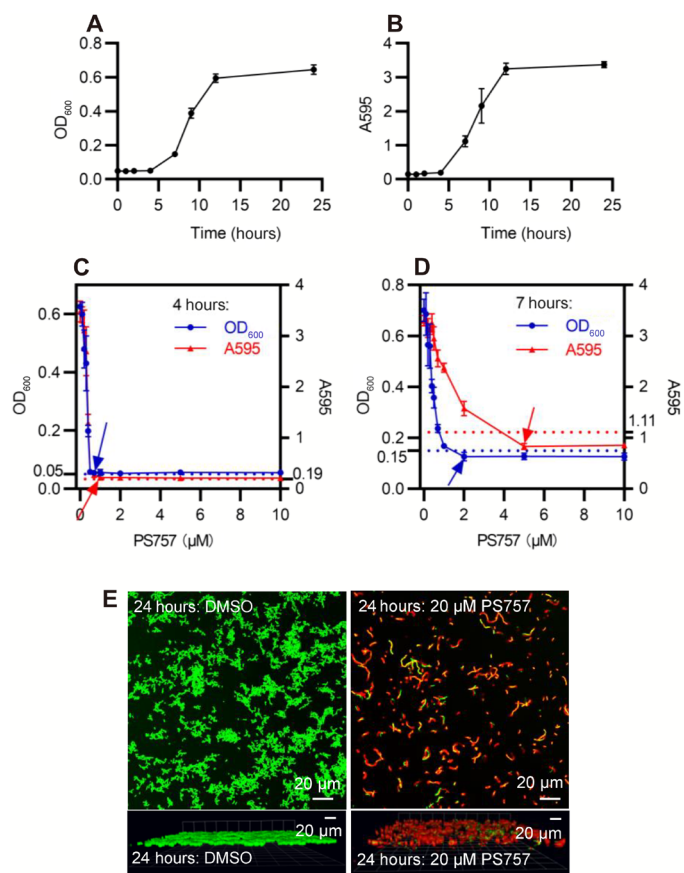

Fig. 2. GmPcide PS757 was active against *S. pyogenes* biofilm. (**A** and **B**) Bacterial growth (A) and biofilm formation (B) of *S. pyogenes* HSC5 strain were measured in microplate assays for 24 hours using BHI medium, which identified 4, 7, and 24 hours as the time points for three different phases of *S. pyogenes* biofilm formation, including biofilm initiation, biofilm development, and fully mature biofilm. (**C**) At 4 hours, PS757 treatment at the concentrations of 0.7 and 1.0 μM prevented *S. pyogenes* HSC5 bacterial growth and biofilm formation in the initiation phase, respectively. (**D**) At 7 hours, PS757 treatment at the concentrations of 2.0 and 5.0 μM ceased *S. pyogenes* HSC5 bacterial growth and biofilm formation in the maturing phase, respectively. (**E**) At 24 hours, PS757 treatment at the bactericidal concentration of 20 μM eradicated mature *S. pyogenes* HSC5 biofilm. OD_{600}, optical density at 600; A595, absorbance at 595.

treatment, infected mice received a subcutaneous injection of PS757 (1.2 mg/kg) or vehicle (DMSO) adjacent to the site of infection at 2, 24, 48, and 70 hours PI (Fig. 3A). When examined over 3 days, GmPcide-treated mice experienced less infection-related weight loss on day 1 and gained more weight over the period of observation (Fig. 3B). By day 3, treated mice also had considerably reduced tissue damage, as shown by a significant decrease in ulcer area as compared to vehicle-treated controls (Fig. 3, C and D), a significant reduction in bacterial burden of approximately 1 log (Fig. 3E), and a reduction in serum levels of pro-inflammatory cytokines tumor necrosis factor–α (TNFα) (Fig. 3F) and interleukin-6 (IL-6) (Fig. 3G), but not IL-1β (Fig. 3H). Immunofluorescence microscopy characterizations of thigh tissue samples from both untreated and treated mice revealed the accumulation of streptococcal and neutrophil cells at the infection site, with elevated amounts observed in the vehicle-treated mice compared with the PS757-treated group (Fig. 3I
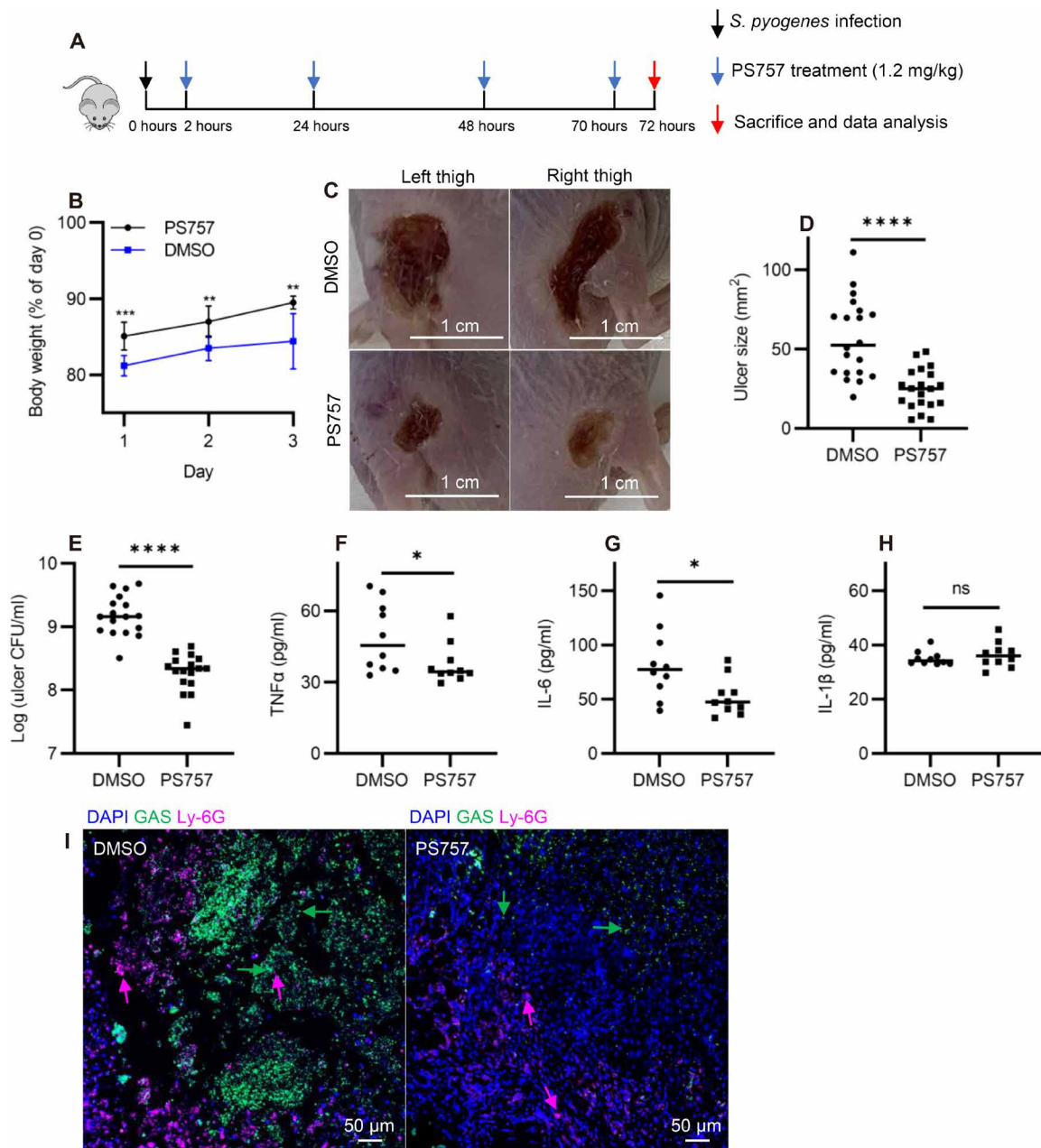
Fig. 3. GmPcide PS757 was effective in treating *S. pyogenes* SSTI in mice. (**A**) Timeline of the 3-day infection and treatment protocol by using PS757 to treat *S. pyogenes* SSTI in mice. (**B**) PS757 treatment alleviated acute weight loss caused by *S. pyogenes* SSTI in mice in 3 days. (**C** and **D**) PS757 treatment reduced ulcer formation at day 3 of *S. pyogenes* SSTI in mice ($P < 0.0001$). (**E**) PS757 treatment attenuated bacterial burden at day 3 of *S. pyogenes* SSTI in mice ($P < 0.0001$). (**F** to **H**) Generation of host pro-inflammatory inflammation cytokines, TNFα [(E) $P \leq 0.05$] and IL-6 [(F) $P \leq 0.05$], but not IL-1β (H), were reduced in the PS757-treated group at day 3 of *S. pyogenes* SSTI in mice. (**I**) Immunofluorescence microscopy characterizations of thigh tissue samples from both vehicle-treated and PS757-treated mice demonstrated the accumulation of streptococcal and neutrophil cells and intensive interaction in between at the infection site, as well as elevated amounts of these cell types in the vehicle-treated mice group. Statistics were performed with Mann-Whitney *U* test. $P \leq 0.05$ is considered as statistically significant. *$P \leq 0.05$, **$P < 0.01$, ***$P < 0.001$, and ****$P < 0.0001$. ns indicates not significant. DAPI, 4′,6-diamidino-2-phenylindole.

and fig. S5). A prior study evaluates subcutaneous injection of several different antibiotics for treatment of *S. pyogenes* SSTI using the murine subcutaneous infection model, with azithromycin showing the most robust efficacy (*21*). Comparison to the current study indicated that GmPcide PS757 was as effective in reducing tissue damage as these standard-of-care antibiotics. Moreover, further investigations can be

directed at examining the ability of GmPcides for increasing inflammation early, and recruiting more neutrophils to the infection site could help to examine whether the drug also have prophylactic potency in treating *S. pyogenes* SSTI, which could be an interesting topic for follow-up. Together, these data show that treatment with GmPcide PS757 has efficacy for improving outcomes over the acute phase of SSTI.

GmPcide PS757 treatment accelerates healing kinetics

To test the effect of GmPcides following the acute phase, mice were treated with PS757 or vehicle alone as described above but were then monitored over a period of 12 days (Fig. 4A). When tissue damage was examined, ulcers in vehicle-treated mice obtained a maximum area at approximately 6 days PI, characterized by the formation of a hard eschar consisting of dry necrotic tissue on the lesion surface (Fig. 4, B and C). In contrast, ulcer area in PS757-treated mice reached maximum area at day 3 and starting from day 2 was significantly smaller than those in vehicle-treated mice (Fig. 4, B and C). Furthermore, while the ulcers in the vehicle control group maintained a relatively constant size, those in the PS757 group diminished in size over the course of 12 days (Fig. 4, B and C). Evidence of accelerated healing in PS757-treated mice came from examination of eschars, where in the vehicle control group, only 21% of eschars (4 of 19 mice) had sloughed off the ulcer surface with new and healthy skin underneath by day 12 (Fig. 4D). In contrast, eschars began sloughing off from PS757-treated mice starting at day 6, and by day 12, 75% of mice had lost their eschars (15 of 20), which were replaced with new and healthy skin (Fig. 4D). While the major effect of GmPcide treatment was on the amelioration of tissue damage, multiple injections of GmPcides over the course of infection did decrease bacterial burdens by an average of 1.3 logs (Fig. 4E).

Since optimization of pharmacokinetics was not the goal of this study, this suggests that GmPcides can be further refined to be even more effective in bacterial clearance. Together, these results demonstrated that PS757 can both limit the degree of tissue damage, as well as accelerate bacterial clearance and wound healing in *S. pyogenes* murine SSTI.

GmPcide PS757 has antivirulence properties

As described above, reduced tissue damage and accelerated wound healing in GmPcide-treated mice did not directly correlate with a reduction in bacterial burdens. This suggests that PS757 has a potent "antivirulence activity" that functions to inhibit the expression of key virulence factors that contribute to tissue damage. This was tested by performing a comparative transcriptomic analysis of bacteria during in vitro culture with a concentration of PS757 that does not inhibit growth. Comparisons were made between cultures in the stationary phase of growth, since prior studies have shown that this condition most closely represents the bulk transcriptome from bacteria in lesions at 3 days PI (*22*, *23*). Following 24 hours of culture in media supplemented with 0.4 μM PS757 or vehicle only (DMSO), RNA was extracted and processed for RNA sequencing (RNA-seq). A principal components analysis (PCA) (*24*) of triplicate samples for each of the PS757 and vehicle only treatment groups showed distinct
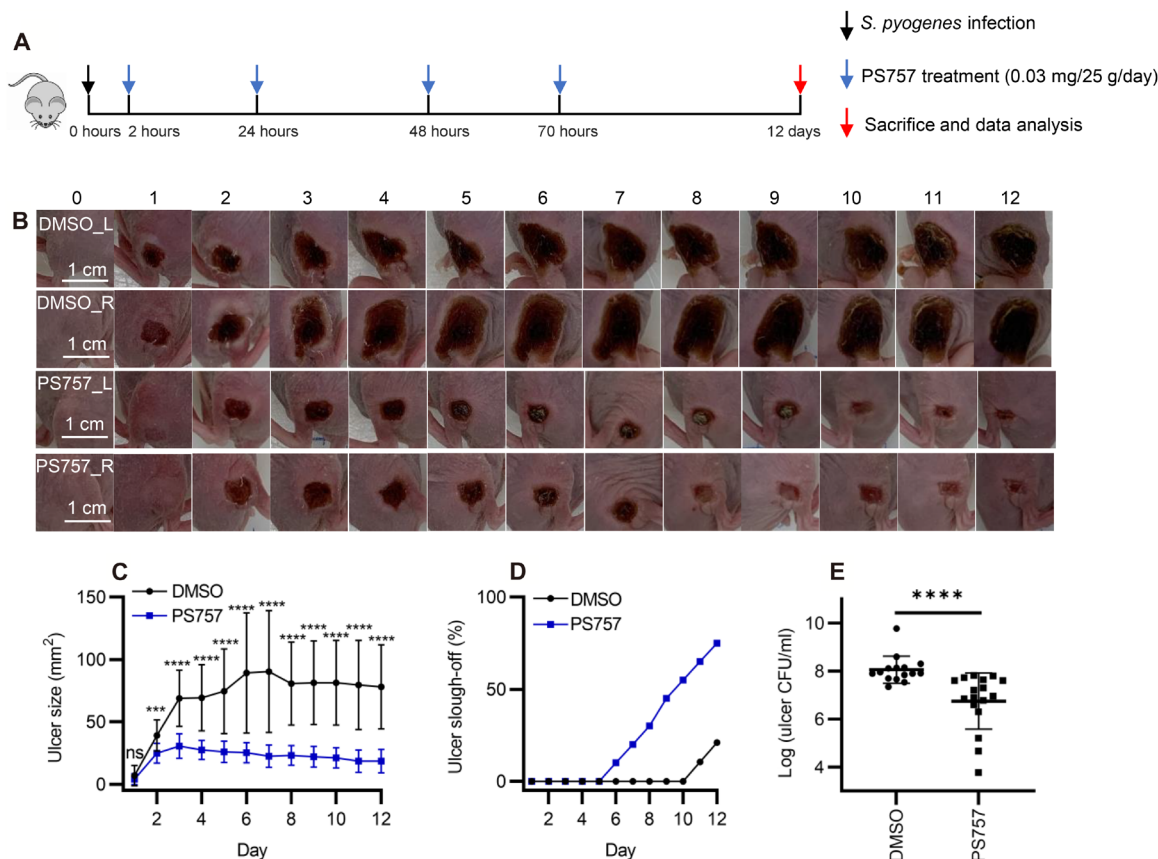

Fig. 4. GmPcide PS757 treatment promoted ulcer healing and bacterial clearance in *S. pyogenes* SSTI in mice. (**A**) Timeline of the 12-day infection and treatment protocol by using PS757 to treat *S. pyogenes* SSTI in mice. (**B** and **C**) PS757 treatment promoted ulcer healing in *S. pyogenes* SSTI in mice during 12 days of infection ($P < 0.001$). (**D**) PS757-treated mice were observed with quicker eschars slough-off from the infected skin than the untreated group in 12-day *S. pyogenes* SSTI in mice. (**E**) PS757 treatment promoted the clearance of bacterial infection at day 12 in *S. pyogenes* SSTI in mice ($P < 0.0001$). Statistics were performed with Mann-Whitney *U* test. $P \leq 0.05$ is considered as statistically significant. ***$P < 0.001$ and ****$P < 0.0001$.

separation (Fig. 5A), demonstrating that PS757 induced distinct transcriptome differences. Analysis of differentially expressed genes (DEGs; |log$_2$(FC)| > 0.5; P < 0.05) (data S1) identified 75 down-regulated genes (50 genes with an annotated protein function and 25 genes annotated as encoding a "hypothetical protein") and 277 up-regulated genes (237 genes with an annotated protein function and 40 genes annotated as encoding a hypothetical protein) (Fig. 5B). Of the most significantly regulated genes (|log$_2$(FC)| and −log(P) > 99% confidence intervals upper limits), nine genes were down-regulated (seven genes with annotated protein function and two genes annotated as encoding a hypothetical protein), and 33 genes were up-regulated (32 genes with annotated protein function and 1 gene annotated as encoding a hypothetical protein) (Fig. 5B and table S3). The group of highly up-regulated genes (fig. S6) featured two ribosomal protein-associated pathways, rps and rpl, which encodes the 30S and the 50S subunits of the bacterial ribosome (70S) that contribute to protein synthesis (*25*). Others include *isaA*, similar to an antigenic, cell wall–associated autolysin *S. aureus*

(*26*, *27*), and *brpA*, a regulator of biofilm function in *Streptococcus mutans* (*15*, *28*). Other up-regulated genes were found to be related to cellular biosynthetic and metabolic processes in general. No key virulence or antibiotic resistance associated determinants of *S. pyogenes* were identified from the highly up-regulated group of genes (fig. S6). The significantly down-regulated gene group identified *emm5* (genomic locus: GPBJDOFB_01691) as the most down-regulated gene (Fig. 5, C and D), which encodes the M protein, a cell wall–associated surface protein that plays multiple roles in *S. pyogenes* infection (*29*, *30*). Another prominently down-regulated gene was *speB* (genomic locus: GPBJDOFB_01704) (Fig. 5B), which encodes a secreted cysteine protease and multifunctional toxin (*31–34*). Analysis by quantitative reverse transcription polymerase chain reaction (RT-qPCR) confirmed that PS757 significantly inhibited expression of *emm5* and *speB* (Fig. 5, E and F) and significantly reduced protease activity in culture supernatants (Fig. 5F). Together, these results indicate that PS757 has antivirulence properties on streptococcal cells exposed to sublethal concentrations
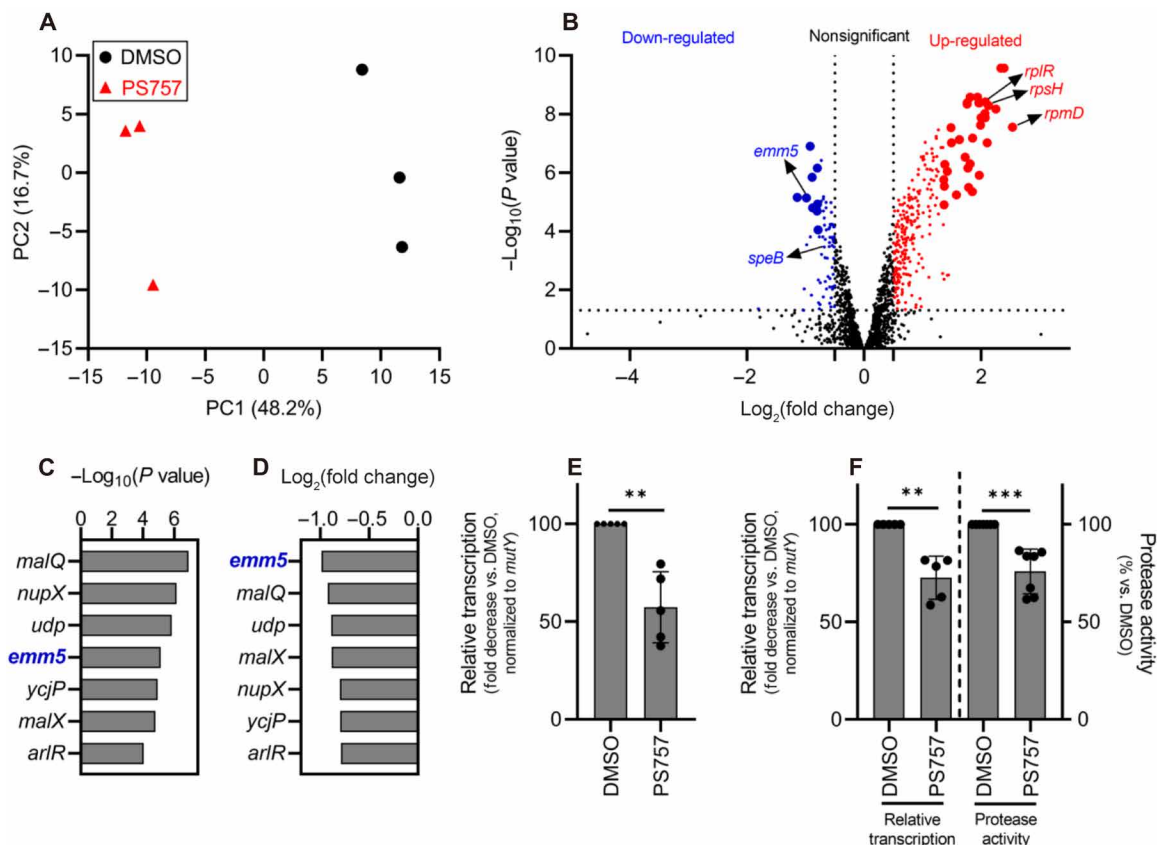

Fig. 5. GmPcide PS757 treatment of *S. pyogenes* resulted in altered transcriptome featuring the inhibition of two major virulence factors (*emm5* and *speB*). (**A**) PCA was conducted for comparing the transcriptomes of *S. pyogenes* HSC5 (obtained from RNA-seq) between two conditions under the treatments of 0.4 μM PS757 or DMSO vehicle. Score plot (PC2 ~ PC1) of the first (PC1) and second (PC2) principal components revealed the transcriptome differences between these two conditions, with clear separation observed along the PC1 axis (accounting for 48.2% of total variance between specimens). (**B**) A volcano plot comparing the PS757-treated versus vehicle (DMSO)-treated was used for identifying DEGs in RNA-seq analysis. DEGs with log$_2$(FC) > 0.5 and P < 0.05, including down- and up-regulated genes, were indicated as blue and red dots, respectively. A more stringent criteria, upper limits of the 99% confidence intervals (CIs) for log$_2$(FC) and −log(P) among DEGs, was further applied to identify the most significant DEGs, with down- and up-regulated genes indicated as bigger blue and red dots, respectively. (**C** to **E**) Seven genes were identified as the most down-regulated group of genes by the two more stringent criteria [(C) and (D)]. Among which, gene *emm5*, a major and multifunctional virulence factor of *S. pyogenes*, was identified with the highest inhibition among all genes by PS757 treatment (D), followed by validation by RT-qPCR test (E). (**F**) Another major *S. pyogenes* virulence factor, *speB*, was also identified with down-regulated transcription induced by PS757 treatment, which was validated by RT-qPCR and protease activity assays. Statistics were performed with Mann-Whitney U test. $P \leq 0.05$ is considered as statistically significant. **P < 0.01 and ***P < 0.001.

that may have contributed to its effective treatment of *S. pyogenes* SSTI in mice.

DISCUSSION

In this study, we found that GmPcide PS757, a member of a novel family of antimicrobial compounds synthesized around a peptidomimetic ring-fused 2-pyridone scaffold, could prevent *S. pyogenes* biofilm formation and effectively treat *S. pyogenes* SSTI in a murine model. Analyses of *S. pyogenes* treated with PS757 revealed antivirulence properties that involved inhibiting the expression of key virulence factors including M protein and the SpeB protease, as well as the induction of nucleoid and cell wall damage. PS757's antivirulence and anti-biofilm activities likely contributed to its efficacy for treatment of *S. pyogenes* SSTI.

In addition to their antivirulence activity, GmPcides are bacteriostatic and/or bactericidal against a broad range of Gram-positive species (5); however, their mechanism of action is unknown. Characterization of activity against *E. faecalis* has shown that GmPcides are bacteriostatic against exponentially growing cells but bactericidal against stationary phase cells (5). This latter mechanism resembles the process of fratricide, where activation of the GelE protease and the ATN autolysin, also known as autolysis A (AtlA), leads to the lysis of a subpopulation of cells to release DNA for the promotion of biofilm formation (35). In the present study, we found that GmPcides were bactericidal against both exponential and stationary phases *S. pyogenes*, revealing its robust bactericidal activity against all phases of streptococcal cells. Moreover, when treated with either sublethal or bactericidal concentrations of PS757, *S. pyogenes* cells were observed with nucleoid abnormalities featuring a condensed and filamentous structure, similar to what has been reported for the fluoroquinolone antibiotic nalidixic acid and the lantibiotic nisin, which can cause DNA condensation and fragmentation by targeting the DNA gyrase in *S. aureus* (19, 36). Exposure of *S. pyogenes* to a bactericidal concentration of PS757 induced cell wall abnormalities with numerous dense globular structures formed at the periphery of the cell wall, which resembles the blisters and bubbles that appear in the cell envelopes of *E. coli* cells that have been treated with the antimicrobial peptide gramicidin S (20). Notably, the mechanism of action and molecule structure of PS757 demonstrated similarities to another antibiotic, daptomycin, which is highly active against *S. pyogenes* and acts by irreversibly binding to the bacterial cell membrane that causes depolarization and thus results in cell death. Daptomycin has been approved in the United States for treating *S. pyogenes* SSTI and no daptomycin-resistant group A streptococcus (GAS) isolate has been reported to date (37–39). In summary, the antimicrobial activity of GmPcide PS757 may be associated with targeting multiple pathways in *S. pyogenes*, including adverse membrane stress caused by inhibition of an essential pathway, including DNA replication (40), cell wall biosynthesis (20, 41), or production of specific proteins (42).

Consistent with other reports that have identified efflux systems as determinants of intrinsic multidrug resistance against both Gram-negative and Gram-positive pathogens, with major facilitator superfamily and resistance nodulation cell division family transporters having the ability to expel a broad range of antimicrobial drugs (43–45), we have also identified efflux systems that contribute to resistance against GmPcides. Examples include lmrB and lmo2589, where mutations that presumably alter their efflux activities contribute to

the development of GmPcide resistance in *E. faecalis* and *Listeria monocytogenes*, respectively. GmPcides with reduced rates of resistance are under active development.

GmPcides are one of only a few classes of antibiotics that can kill nondividing bacterial cells (5). Here, we show that they also are one of the few antibiotics that are effective at killing cells in biofilm. It has been shown that up to 90% of *S. pyogenes* strains collected from both invasive and noninvasive infections were able to form biofilm (46). *S. pyogenes* can form biofilm on a variety of host surfaces and tissues following a complexed process involving four development stages, including the cell attachment, microcolony formation, maturation, and biofilm dispersal, and that cells residing within the biofilm matrix exhibit higher antibiotic resistance (47). Biofilm-associated *S. pyogenes* infections often result in persistent host carriage and recurrent infections and are a major reason leading to treatment failure following therapy with available standard-of-care antibiotics (14, 46, 48). Moreover, numerous virulence factors, including the SpeB cysteine protease, are up-regulated in biofilm, suggesting biofilm potentially enhances pathogenesis (13, 22). Thus, the capability of PS757 to effectively inhibit biofilm formation at all developmental stages, together with its robust antimicrobial potency against both exponentially dividing and stationarily nondividing cells, may have played a role in its ability to treat *S. pyogenes* SSTI.

The ability of PS757 to inhibit expression of the SpeB toxin and expression of other virulence factors may also have contributed to its efficacy in treatment of SSTI. Toxins are thought to play an important role in the tissue damage that accompanies SSTI, and this is the basis for therapies that combine a bactericidal β-lactam antibiotic with clindamycin or the newly discovered 2S-alkyne, which have been shown to inhibit toxin expression in vitro (31, 49–53). The mechanism of clindamycin inhibition of toxin expression may involve its ability to alter the expression of several regulators of toxin transcription (54). While the mechanism through which GmPcides inhibit *S. pyogenes* virulence factor expression is unknown, it has been shown that a GmPcide-related compound can alter the activity of PrfA, a transcriptional regulator of virulence factor expression in *L. monocytogenes* (55, 56). It is known that regulation of virulence in *S. pyogenes* is multifactorial, involving transcriptional factors that respond to nutrient availability, chemical stressors, temperature, oxygen host immune components, and stress-related responses (57–60). Whether GmPcides directly target transcription regulators, induce a stress-related response, or both to regulate virulence in *S. pyogenes* remains to be determined. Notably, the therapeutic approach by combining β-lactam antibiotics with clindamycin is being rendered less effective by rising rates of clindamycin resistance. Another approach has been to use passive immunotherapy with intravenous pooled human immunoglobulin (53), which may both neutralize toxins and promote neutralization of antiphagocytic and biofilm-promoting virulence factors such as M protein. Thus, the ability of GmPcides to inhibit expression of SpeB, M protein, and other virulence factors may have contributed to PS757's ability to treat SSTI by reducing tissue damage, accelerating bacterial clearance, stimulating ulcer healing, and alleviating host inflammation to promote a quicker recovery. Overall, these results demonstrate that GmPcides hold great promise in preventing and treating *S. pyogenes* SSTI. Our findings will help direct the continuing development and optimization of GmPcide compounds toward a novel class of antibiotics.

MATERIALS AND METHODS

Ethics statement
All animal experimentation in this study was conducted following the National Institutes of Health guidelines for housing and care of laboratory animals and performed in accordance with institutional regulations after pertinent review and approval by the Animal Studies Committee at Washington University School of Medicine (protocol #22-0307).

Bacterial strains, culture, and GmPcide
All experiments described used *S. pyogenes* HSC5 (originally obtained from H.S. Courtney, University of Tennessee, Memphis), a M14 serotype strain with no known antibiotic resistance, whose genome has been determined (*22, 61–63*). This strain is robustly expresses the SpeB cysteine, and its virulence has been extensively characterized in several different experimental models, including the murine SSTI model (*8, 9*). Unless otherwise specified, liquid cultures used C medium (*22*) and were inoculated from several colonies picked from a C medium plate that had been incubated overnight at 37°C under the anaerobic conditions produced by a commercial anaerobic generator (Becton Dickinson, 260683). Routine liquid culture was performed using 15-ml conical tubes containing 10 mls of media that were incubated under static conditions at 37°C. GmPcide PS757 was synthesized from a 2-pyridone scaffold with as previously reported (*5*) and was chosen for further studies in the current work.

Determination of MIC and MBC
The MIC and MBC represent the lowest concentrations of GmPcides and antibiotics that inhibited growth and viability, respectively. The MIC and MBC concentrations for GmPcide PS757 and four types of standard-of-care antibiotics (*21, 64*)—including penicillin (GOLDBIO, P-304-50), cefotaxime (GOLDBIO, C-104-1), vancomycin (GOLDBIO, V-200-25), and azithromycin (MilliporeSigma, PHR1088)—were examined by the broth microdilution MIC and MBC assays using BHI medium following the methods established by the Clinical and Laboratory Standards Institute (*5, 65*).

Determination of antimicrobial synergy
The antimicrobial synergy of GmPcide PS757 with four antibiotics—e.g., penicillin (GOLDBIO, P-304-50), cefotaxime (GOLDBIO, C-104-1), vancomycin (GOLDBIO, V-200-25), and azithromycin (MilliporeSigma, PHR1088)—was examined by checkerboard method and E test as previously described (*5, 66, 67*). Briefly, the checkerboard assay was performed to examine the antimicrobial activity of two antimicrobial compounds in combination at a series of concentrations following a 1:2 dilution across a 96-well plate. Fractional inhibitory concentration index (FICI) was calculated by the E test as: $\text{FICI} = (\text{MIC}_{AB}/\text{MIC}_A) + (\text{MIC}_{BA}/\text{MIC}_B)$. MIC_{AB} is the MIC of drug A tested in combination, and MIC_A is the MIC of drug A tested alone. Similarly, MIC_{BA} is the MIC of drug B tested in combination, and MIC_B is the MIC of drug B tested alone. Synergy is defined as $\text{FICI} \leq 0.5$, indifference is defined as $0.5 < \text{FICI} \leq 4$, and antagonism is defined as $\text{FICI} > 4$.

Determination of GmPcide bactericidal activity against exponential and stationary *S. pyogenes*
Cells from an overnight culture grown described above were harvested by centrifugation, washed with an equal volume of sterile saline (MilliporeSigma, S8776), and resuspended to equal volume of fresh sterile saline. This suspension was used to inoculate fresh C-medium at a dilution of 1:1000 that was then dispensed at 200-µl aliquots into the wells of a 96-well plate (*22*). At 7 and 14 hours after inoculation, exponential and stationary *S. pyogenes* cells were treated with vehicle alone (DMSO) (Sigma-Aldrich, D2650) or with PS757 (20 µM) for an additional 12 hours of incubation, and CFUs were enumerated by quantitative plating.

Determination of sublethal GmPcide concentrations
Cells from an overnight culture grown described above were harvested by centrifugation, washed with an equal volume of sterile saline (MilliporeSigma, S8776), and resuspended to equal volume of fresh sterile saline. This suspension was used to inoculate fresh C-medium at a dilution of 1:1000 that was then dispensed at 200-µl aliquots into the wells of a 96-well plate to which GmPcide PS757 was added at concentrations ranging from 0 to 5.0 µM. The OD_{600} of the culture was measured using a spectrophometer (Beckman Coulter, DU-800) over the course of 24 hours, and CFUs were enumerated by quantitative plating. The highest functional sublethal GmPcide concentration was determined as the highest concentration of one antimicrobial agent that does not inhibit the streptococcal cells growth.

Electron microscopy
Using the microplate assay described above, streptococci were cultured with a sublethal (0.4 µM) concentration of PS757 for 24 hours or were exposed to a bactericidal concentration by first culturing cells in the absence of GmPcide overnight, followed by the addition of PS757 (20 µM) and continuing the incubation for an additional 5 hours. Cells were prepared and examined using TEM as described in detail (*68–71*). Briefly, cells were harvested by centrifugation and fixed by the addition 2% paraformaldehyde/2.5% glutaraldehyde (Polysciences Inc.) in 100 mM sodium cacodylate buffer (pH 7.2) to the bacterial pellet for 1 hour at room temperature. Samples were washed in sodium cacodylate buffer and postfixed in 1% osmium tetroxide (Polysciences Inc.) for 1 hour and then rinsed in deionized water before en bloc staining with 1% aqueous uranyl acetate (Ted Pella Inc.) for 1 hour. Following several deionized water rinses, samples were dehydrated in a graded series of ethanol and embedded in Eponate 12 resin (Ted Pella Inc.). Sections of 95 nm were cut with a Leica Ultracut UCT ultramicrotome (Leica Microsystems Inc.), stained with uranyl acetate and lead citrate, and visualized on a JEOL 1200 EX transmission electron microscope (JEOL USA Inc.) equipped with an AMT 8 megapixel digital camera and AMT Image Capture Engine V602 software (Advanced Microscopy Techniques).

Confocal microscopy
Using the microplate assay described above, streptococci were first cultured in the absence of GmPcide overnight, followed by the addition of PS757 (20 µM) or vehicle (DMSO) and additional incubation for 5 hours. Cells were prepared and examined using fluorescence confocal microscopy (*72*). Briefly, cells were harvested by centrifugation, washed with and resuspended in saline (MilliporeSigma, S8776), stained with Nile Red (5 µg/ml; Invitrogen, N1142) for 1 hour, washed with and resuspended in saline, mounted on microscopy slide (VWR) using Prolong Gold (Invitrogen, P36935), and visualized using a Zeiss LSM 880 Confocal Laser Scanning Microscope, as previously described (*73–75*).

Biofilm culture and quantitation

Culture in 96-well plates in BHI medium (Thermo Fisher BD, DF0037-07-0) at 37°C were monitored for planktonic growth and biofilm formation by OD_{600} and staining with CV (68, 69, 76), respectively. For the latter, planktonic culture was removed by aspiration, and the wells were stained with a 0.5% CV solution for 10 min, washed with deionized water, air-dried on absorbent paper overnight, and extracted with 33% acetic acid (Sigma-Aldrich, 695092) for 10 min. Extracts were then diluted 20-fold (in 33% acetic acid), and their absorbance at 595 nm was determined using a spectrophotometer (Beckman Coulter, DU-800).

GmPcide treatment of biofilm

Characterization of biofilm cultures indicated that *S. pyogenes* HSC5 biofilm in BHI medium had three distinct phases, initiation, development, and maturation, which occurred at 4, 7, and 24 hours after inoculation, respectively (Fig. 2B). GmPcide antibiofilm activity was then determined by the addition of PS757 as follows (fig. S3, A to C): At 4 and 7 hours, PS757 was added to 96-well plate cultures at concentrations ranging from 0 to 20 µM. At 12 hours after inoculation, planktonic and biofilm growth was measured, as described above. For mature biofilm, cultures were prepared using 5 ml of medium in a 35-mm-diameter culture dish (MatTek, P35G-0-14-C). At 24 hours after inoculation, cultures were treated with vehicle alone (DMSO) (Sigma-Aldrich, D2650) or with PS757 (20 µM) for an additional 5 hours of incubation. Bacterial viability was then assessed by confocal microscopy using a LIVE/DEAD fluorescent probe (Thermo Fisher Scientific, L7012). Following 30 min of staining, plates were washed with saline and imaged using a Zeiss LSM 880 Confocal Laser Scanning Microscope, as previously described (73–75).

Subcutaneous mouse infection and GmPcide treatment

Subcutaneous murine infection was conducted as previously described (8–11) with the following modifications: For 3-day infections, seven-week-old female SKH1 hairless mice (Charles River Laboratories) were injected subcutaneously with 10^7 CFU into both the left and right rear thighs, followed by four treatments by subcutaneous injection of vehicle (DMSO) or PS757 (1.2 mg/kg body weight, dissolved in DMSO) adjacent to the site of infection at 2, 24, 48, and 70 hours PI. The body weight of each mouse was recorded daily, and ulcers were quantified by digital photography and ImageJ software, as described (9, 77). On day 3, blood was collected using submandibular vein (cheek pouch) method into a collection tube (BD Microtainer, 365967) (78). Samples were subjected to centrifugation to obtain serum, and levels of selected cytokines were quantitated using the DuoSet ELISA kits (79), including TNFα (R&D Systems, DY410), IL-6 (R&D Systems, DY406), and IL-1β (R&D Systems, DY401). Mice were euthanized on day 3, ulcers were resected, and bacterial CFUs were determined from tissue homogenates as described (9). Initiation of 12-day infection and treatments were conducted as described in the 3-day protocol, no additional treatments were performed, and the infection was monitored over the course of 12 days. The data presented are representative of at least two independent experiments, each of which was conducted with 10 mice in each experimental group.

Histopathology and immunofluorescence

Histopathological characterization of infected tissue was conducted as previously described (79–82). Briefly, ulcers and surrounding tissue were excised and stored in 10% neutral-buffered formalin solution (Sigma-Aldrich, HT5012) for no more than 3 days. Tissue samples were washed in phosphate-buffered saline, fixed in methacarn (60% methanol, 30% chloroform, and 10% glacial acetic acid), embedded in paraffin, and then sectioned. The resulting tissue sections were dewaxed in xylene and ethanol (100, 95, and 70%), followed by an antigen retrieval step using 10 mM sodium citrate solution with 0.05% Tween 20 at pH 6.0 and blocked in 5% bovine serum albumin solution (Sigma-Aldrich, 05470). Sections were stained with 4′,6-diamidino-2-phenylindole (Invitrogen, P36935) to reveal nuclei and fluorescent antibody conjugates to stain: (i) neutrophils with Ly-6G (BioLegend, 127610) and (ii) bacteria with an anti-*Streptococcus* group A polyclonal antibody (Invitrogen, PA1-73056). Staining was visualized using a Zeiss Axio Imager M2 immunofluorescence microscope.

RNA sequencing

Microplate (96-well) culture in C medium was conducted as described above with the addition of 0.4 µM PS757 or vehicle (DMSO). At 24 hours, multiple wells were harvested and pooled for further processing, with the experiment repeated in triplicate. Extraction of RNA used the Direct-zol RNA Miniprep Plus Kit (Zymo Research, R2072) with the quality of the purified RNA determined by spectroscopy (NanoDrop 2000, Thermo Fisher Scientific). Libraries for Illumina sequencing were prepared using the FastSelect RNA Kit (QIAGEN, 334222), according to the manufacturer's protocol, and sequences were determined using an Illumina NovaSeq 6000. Basecalls and demultiplexing were performed with Illumina's bcl2fastq software and a custom python demultiplexing program with a maximum of one mismatch in the indexing read. RNA-seq reads were then aligned to the Ensembl release 101 primary assembly with STAR version 2.7.9a (83). Gene counts were derived from the number of uniquely aligned unambiguous reads by Subread:featureCount version 2.0.3 (84). The isoform expression of known Ensembl transcripts were quantified with Salmon version 1.5.2 (85) and assessed for the total number of aligned reads, total number of uniquely aligned reads, and features detected. The ribosomal fraction, known junction saturation, and read distribution over known gene models were quantified with RSeQC version 4.0 (86).

Comparative transcriptomic analysis

All gene counts obtained from RNA-seq were then imported into the R/Bioconductor package EdgeR (87), and TMM normalization size factors were calculated to adjust for differences in library size. Ribosomal genes and genes not expressed in the smallest group size minus one sample greater than one count per million were excluded from further analysis. The TMM size factors and the matrix of counts were then imported into the R/Bioconductor package Limma (88). Weighted likelihoods based on the observed mean-variance relationship of every gene and sample were calculated for all samples, and the count matrix was transformed to moderated $\log_2$ counts per million with Limma's voomWithQualityWeights (89). The performance of all genes was assessed with plots of the residual SD of every gene to their average log count with a robustly fitted trend line of the residuals. Differential expression analysis was then performed to analyze for differences between conditions with results filtered for only those genes with Benjamini-Hochberg false discovery rate–adjusted P values less than or equal to 0.05. A PCA was performed on differential expression data to distinguish differences between conditions (68). To find the significantly regulated

Table 2. Primers list.

Gene	Sequence (5′-3′)
emm5 forward	CAAGAACAAGCAGAAGCAC
emm5 reverse	GTCTTACTCCGTTGTTCTAAGTC
speB forward	GTTAACTTAGGTGGAGAACTTTC
speB reverse	CTTTGATTTGTTCGACATAAC
mutYF forward	GAAATCATGTTGCAACAAAC
mutYR reverse	CAAAATCAACCATCACTTG

genes, the Limma voomWithQualityWeights transformed $\log_2$ counts per million expression data were then analyzed via weighted gene correlation network analysis (WGCNA) with the R/Bioconductor package WGCNA (*90*). Briefly, all genes were correlated across each other by Pearson correlations and clustered by expression similarity into unsigned modules using a power threshold empirically determined from the data. An eigengene was then created for each de novo cluster, and its expression profile was then correlated across all coefficients of the model matrix. Because these clusters of genes were created by expression profile rather than known functional similarity, the clustered modules were given the names of random colors where gray is the only module that has any pre-existing definition of containing genes that do not cluster well with others. The information for all clustered genes for each module was then combined with their respective statistical significance results from Limma to determine whether or not those features were also found to be significantly differentially expressed.

Quantitative reverse transcription polymerase chain reaction

RNA was prepared as described above, with five replicates collected for each treatment condition. Reverse transcription used iScript Reverse Transcription Supermix (Bio-Rad, 1708840) with the thermocycler (Applied Biosystems, A24812) programmed as follows: (i) priming for 5 min at 25°C, (ii) RT for 20 min at 25°C, and (iii) RT inactivation for 1 min at 95°C to acquire cDNA. After reverse transcription, 12.5 ng of cDNA was mixed with primers specific to each gene (Table 2), and PCR was conducted using the iTaq Universal SYBR Green Supermix as recommended by the manufacturer (Bio-Rad, 1725121). All qPCR assays were performed on a CFX96 Real-Time System (Bio-Rad) using the following protocol: a 5-min polymerase activation and DNA denaturation at 95°C, another 10-s DNA denaturation at 95°C, 30 cycles of a 30-s annealing at 60°C, and ending with a melt curve with 5 s at 65°C first and 5 s each at a 0.5°C increase between 65° and 95°C, with threshold cycles (Ct) obtained at the end of the reactions. Each sample was run in triplicate with average Ct values calculated. Relative expression compared to control was determined by the ΔΔCt method (*91*).

Protease assay

SpeB is secreted by *S. pyogenes* as an inactive 40-kDa zymogen that is converted into a 28-kDa active protease by autocatalytic cleavage or other host and streptococcal proteases (*58*). The activity of active SpeB in the extracellular space of *S. pyogenes* was measured by digestion of casein using a microplate method as previously described

(*23*, *92*, *93*). Microplate culture was performed as described above in C medium with the addition of 0.4 µM PS757 or vehicle (DMSO). After 24 hours, extracellular protease activity was determined in bacterial culture supernatant by a method that measures the increase in relative fluorescence generated by the proteolytic cleavage of fluorescein isothiocyanate–casein (Sigma-Aldrich, C0528). Uninoculated C medium was used to determine background values.

Statistics

Unless otherwise stated, conclusions were based on the comparison of means generated from at least three technical and three biological replicates that were tested for significance using Mann Whitney U test and conducted using GraphPad Prism 9.0 (GraphPad software). $P \leq 0.05$ was considered significant.

Supplementary Materials

This PDF file includes:
Figs. S1 to S6
Tables S1 to S3

Other Supplementary Material for this manuscript includes the following:
Data S1

REFERENCES AND NOTES

1. A. Cassini, L. D. Högberg, D. Plachouras, A. Quattrocchi, A. Hoxha, G. S. Simonsen, M. Colomb-Cotinat, M. E. Kretzschmar, B. Devleesschauwer, M. Cecchini, D. A. Ouakrim, T. C. Oliveira, M. J. Struelens, C. Suetens, D. L. Monnet; Burden of AMR Collaborative Group, Attributable deaths and disability-adjusted life-years caused by infections with antibiotic-resistant bacteria in the EU and the European Economic Area in 2015: A population-level modelling analysis. *Lancet Infect. Dis.* **19**, 56–66 (2019).
2. Antimicrobial Resistance Collaborators, Global burden of bacterial antimicrobial resistance in 2019: A systematic analysis. *Lancet* **399**, 629–655 (2022).
3. L. L. Silver, Challenges of antibacterial discovery. *Clin. Microbiol. Rev.* **24**, 71–109 (2011).
4. S. J. Baker, D. J. Payne, R. Rappuoli, E. De Gregorio, Technologies to address antimicrobial resistance. *Proc. Natl. Acad. Sci. U.S.A.* **115**, 12887–12895 (2018).
5. T. M. Nye, H. Tukenmez, P. Singh, A. L. Flores-Mireles, C. L. P. Obernuefemann, J. S. Pinkner, S. Sarkar, M. Bonde, A. E. G. Lindgren, K. W. Dodson, J. Johansson, F. Almqvist, M. G. Caparon, S. J. Hultgren, Ring-fused 2-pyridones effective against multidrug-resistant Gram-positive pathogens and synergistic with standard-of-care antibiotics. *Proc. Natl. Acad. Sci. U.S.A.* **119**, e2210912119 (2022).
6. CDC, "Antibiotic Resistance Threats in the United States, 2019 (U.S. Department of Health and Human Services, CDC, 2019); http://dx.doi.org/10.15620/cdc:82532.
7. J. R. Carapetis, A. C. Steer, E. K. Mulholland, M. Weber, The global burden of group A streptococcal diseases. *Lancet Infect. Dis.* **5**, 685–694 (2005).
8. M. E. Watson Jr., M. N. Neely, M. G. Caparon, Animal models of *Streptococcus pyogenes* infection, in *Streptococcus pyogenes: Basic Biology to Clinical Manifestations*, D. L. S. Joseph J. Ferretti, Vincent A. Fischetti, Ed. (University of Oklahoma Health Sciences Center, 2016).
9. E. Paluscio, M. E. Watson Jr., M. G. Caparon, CcpA coordinates growth/damage balance for *Streptococcus pyogenes* pathogenesis. *Sci. Rep.* **8**, 14254 (2018).

10. C. C. Kietzman, M. G. Caparon, CcpA and LacD.1 affect temporal regulation of *Streptococcus pyogenes* virulence genes. *Infect. Immun.* **78**, 241–252 (2010).

11. C. C. Kietzman, M. G. Caparon, Distinct time-resolved roles for two catabolite-sensing pathways during *Streptococcus pyogenes* infection. *Infect. Immun.* **79**, 812–821 (2011).

12. J. P. Burnham, M. H. Kollef, Treatment of severe skin and soft tissue infections: A review. *Curr. Opin. Infect. Dis.* **31**, 113–119 (2018).

13. R. C. H. Christie Young, Lily Dubois, Sean D. Reid, *Streptococcus pyogenes* Biofilm in *Streptococcus pyogenes: Basic Biology to Clinical Manifestations*, D. L. S. Joseph J. Ferretti, Vincent A. Fischetti, Ed. (University of Oklahoma Health Sciences Center, 2016).

14. T. Fiedler, T. Koller, B. Kreikemeyer, *Streptococcus pyogenes* biofilms-formation, biology, and clinical relevance. *Front. Cell. Infect. Microbiol.* **5**, 15 (2015).

15. C. Alves-Barroco, J. Paquete-Ferreira, T. Santos-Silva, A. R. Fernandes, Singularities of pyogenic streptococcal biofilms-from formation to health implication. *Front. Microbiol.* **11**, 584947 (2020).

16. A. F. Johnson, C. N. LaRock, Antibiotic treatment, mechanisms for failure, and adjunctive therapies for infections by group A streptococcus. *Front. Microbiol.* **12**, 760255 (2021).

17. T. Ikebe, K. Hirasawa, R. Suzuki, J. Isobe, D. Tanaka, C. Katsukawa, R. Kawahara, M. Tomita, K. Ogata, M. Endoh, R. Okuno, H. Watanabe, Antimicrobial susceptibility survey of *Streptococcus pyogenes* isolated in Japan from patients with severe invasive group A streptococcal infections. *Antimicrob. Agents Chemother.* **49**, 788–790 (2005).

18. B. P. White, E. A. Siegrist, Increasing clindamycin resistance in group A streptococcus. *Lancet Infect. Dis.* **21**, 1208–1209 (2021).

19. C. Jensen, H. Li, M. Vestergaard, A. Dalsgaard, D. Frees, J. J. Leisner, Nisin damages the septal membrane and triggers DNA condensation in methicillin-resistant *Staphylococcus aureus*. *Front. Microbiol.* **11**, 1007 (2020).

20. M. Hartmann, M. Berditsch, J. Hawecker, M. F. Ardakani, D. Gerthsen, A. S. Ulrich, Damage of the bacterial cell envelope by antimicrobial peptides gramicidin S and PGLa as revealed by transmission and scanning electron microscopy. *Antimicrob. Agents Chemother.* **54**, 3132–3142 (2010).

21. N. Barg, Comparison of four antibiotics in a murine model of necrotizing cutaneous infections caused by toxigenic *Streptococcus pyogenes* and *Staphylococcus aureus*. *J. Antimicrob. Chemother.* **42**, 257–260 (1998).

22. K. H. Cho, M. G. Caparon, Patterns of virulence gene expression differ between biofilm and tissue communities of *Streptococcus pyogenes*. *Mol. Microbiol.* **57**, 1545–1556 (2005).

23. J. A. Loughman, M. Caparon, Regulation of SpeB in *Streptococcus pyogenes* by pH and NaCl: A model for in vivo gene expression. *J. Bacteriol.* **188**, 399–408 (2006).

24. Z. Zou, J. I. Robinson, L. K. Steinberg, J. P. Henderson, Uropathogenic *Escherichia* coli wield enterobactin-derived catabolites as siderophores. *J. Biol. Chem.* **300**, 105554 (2023).

25. K. Byrgazov, O. Vesper, I. Moll, Ribosome heterogeneity: Another level of complexity in bacterial translation regulation. *Curr. Opin. Microbiol.* **16**, 133–139 (2013).

26. U. Lorenz, K. Ohlsen, H. Karch, M. Hecker, A. Thiede, J. Hacker, Human antibody response during sepsis against targets expressed by methicillin resistant *Staphylococcus aureus*. *FEMS Immunol. Med. Microbiol.* **29**, 145–153 (2000).

27. M. R. Stapleton, M. J. Horsburgh, E. J. Hayhurst, L. Wright, I. M. Jonsson, A. Tarkowski, J. F. Kokai-Kun, J. J. Mond, S. J. Foster, Characterization of IsaA and SceD, two putative lytic transglycosylases of *Staphylococcus aureus*. *J. Bacteriol.* **189**, 7316–7325 (2007).

28. J. P. Bitoun, S. Liao, X. Yao, S. J. Ahn, R. Isoda, A. H. Nguyen, L. J. Brady, R. A. Burne, J. Abranches, Z. T. Wen, BrpA is involved in regulation of cell envelope stress responses in *Streptococcus mutans*. *Appl. Environ. Microbiol.* **78**, 2914–2922 (2012).

29. W. R. Maxted, The indirect bactericidal test as a means of identifying antibody to the M antigen of *Streptococcus pyogenes*. *Br. J. Exp. Pathol.* **37**, 415–422 (1956).

30. H. R. Frost, M. Sanderson-Smith, M. Walker, A. Botteaux, P. R. Smeesters, Group A streptococcal M-like proteins: From pathogenesis to vaccine potential. *FEMS Microbiol. Rev.* **42**, 193–204 (2018).

31. J. L. Woehl, S. Kitamura, N. Dillon, Z. Han, L. J. Edgar, V. Nizet, D. W. Wolan, An irreversible inhibitor to probe the role of *Streptococcus pyogenes* cysteine protease SpeB in evasion of host complement defenses. *ACS Chem. Biol.* **15**, 2060–2069 (2020).

32. D. C. Nelson, J. Garbe, M. Collin, Cysteine proteinase SpeB from *Streptococcus pyogenes*—A potent modifier of immunologically important host and bacterial proteins. *Biol. Chem.* **392**, 1077–1088 (2011).

33. M. J. Walker, T. C. Barnett, J. D. McArthur, J. N. Cole, C. M. Gillen, A. Henningham, K. S. Sriprakash, M. L. Sanderson-Smith, V. Nizet, Disease manifestations and pathogenic mechanisms of Group A Streptococcus. *Clin. Microbiol. Rev.* **27**, 264–301 (2014).

34. C. Chiang-Ni, J. J. Wu, Effects of streptococcal pyrogenic exotoxin B on pathogenesis of *Streptococcus pyogenes*. *J. Formos. Med. Assoc.* **107**, 677–685 (2008).

35. V. C. Thomas, Y. Hiromasa, N. Harms, L. Thurlow, J. Tomich, L. E. Hancock, A fratricidal mechanism is responsible for eDNA release and contributes to biofilm development of *Enterococcus faecalis*. *Mol. Microbiol.* **72**, 1022–1036 (2009).

36. A. R. Pereira, P. Reed, H. Veiga, M. G. Pinho, The Holliday junction resolvase RecU is required for chromosome segregation and DNA damage repair in *Staphylococcus aureus*. *BMC Microbiol.* **13**, 18 (2013).

37. V. Cattoir, in *Streptococcus pyogenes: Basic Biology to Clinical Manifestations*, D. L. S. Joseph J. Ferretti, Vincent A. Fischetti, Ed. (University of Oklahoma Health Sciences Center, 2022).

38. R. E. Hancock, Mechanisms of action of newer antibiotics for Gram-positive pathogens. *Lancet Infect. Dis.* **5**, 209–218 (2005).

39. I. P. A. King, I. Phillips, In vitro activity of daptomycin against 514 Gram-positive aerobic clinical isolates. *J. Antimicrob. Chemother.* **48**, 219–223 (2001).

40. D. C. Hooper, G. A. Jacoby, Topoisomerase inhibitors: Fluoroquinolone mechanisms of action and resistance. *Cold Spring Harb. Perspect. Med.* **6**, a025320 (2016).

41. P. Sarkar, V. Yarlagadda, C. Ghosh, J. Haldar, A review on cell wall synthesis inhibitors with an emphasis on glycopeptide antibiotics. *Medchemcomm* **8**, 516–533 (2017).

42. S. Arenz, D. N. Wilson, Bacterial protein synthesis as a target for antibiotic inhibition. *Cold Spring Harb. Perspect. Med.* **6**, a025361 (2016).

43. B. D. Schindler, G. W. Kaatz, Multidrug efflux pumps of Gram-positive bacteria. *Drug Resist. Updat.* **27**, 1–13 (2016).

44. X. Z. Li, P. Plesiat, H. Nikaido, The challenge of efflux-mediated antibiotic resistance in Gram-negative bacteria. *Clin. Microbiol. Rev.* **28**, 337–418 (2015).

45. A. Sharma, V. K. Gupta, R. Pathania, Efflux pump inhibitors for bacterial pathogens: From bench to bedside. *Indian J. Med. Res.* **149**, 129–145 (2019).

46. L. Baldassarri, R. Creti, S. Recchia, M. Imperi, B. Facinelli, E. Giovanetti, M. Pataracchia, G. Alfarone, G. Orefici, Therapeutic failures of antibiotics used to treat macrolide-susceptible *Streptococcus pyogenes* infections may be due to biofilm formation. *J. Clin. Microbiol.* **44**, 2721–2727 (2006).

47. D. Viszwapriya, G. A. Subramenium, U. Prithika, K. Balamurugan, S. K. Pandian, Betulin inhibits virulence and biofilm of *Streptococcus pyogenes* by suppressing ropB core regulon, sagA and dltA. *Pathog. Dis.* **74**, ftw088 (2016).

48. S. Brouwer, T. Rivera-Hernandez, B. F. Curren, N. Harbison-Price, D. M. P. De Oliveira, M. G. Jespersen, M. R. Davies, M. J. Walker, Pathogenesis, epidemiology and control of Group A Streptococcus infection. *Nat. Rev. Microbiol.* **21**, 431–447 (2023).

49. F. Andreoni, C. Zurcher, A. Tarnutzer, K. Schilcher, A. Neff, N. Keller, E. Marques Maggio, C. Poyart, R. A. Schuepbach, A. S. Zinkernagel, Clindamycin affects group A Streptococcus virulence factors and improves clinical outcome. *J Infect Dis* **215**, 269–277 (2017).

50. M. Minami, T. Kamimura, M. Isaka, I. Tatsuno, M. Ohta, T. Hasegawa, Clindamycin-induced CovS-mediated regulation of the production of virulent exoproteins streptolysin O, NAD glycohydrolase, and streptokinase in *Streptococcus pyogenes*. *Antimicrob. Agents Chemother.* **54**, 98–102 (2010).

51. J. Sawai, T. Hasegawa, T. Kamimura, A. Okamoto, D. Ohmori, N. Nosaka, K. Yamada, K. Torii, M. Ohta, Growth phase-dependent effect of clindamycin on production of exoproteins by *Streptococcus pyogenes*. *Antimicrob. Agents Chemother.* **51**, 461–467 (2007).

52. D. L. Stevens, A. E. Gibbons, R. Bergstrom, V. Winn, The Eagle effect revisited: Efficacy of clindamycin, erythromycin, and penicillin in the treatment of streptococcal myositis. *J Infect Dis* **158**, 23–28 (1988).

53. D. Laho, S. Blumental, A. Botteaux, P. R. Smeesters, Invasive group A Streptococcal infections: Benefit of clindamycin, intravenous immunoglobulins and secondary prophylaxis. *Front. Pediatr.* **9**, 697938 (2021).

54. B. Henrichfreise, I. Wiegand, I. Luhmer-Becker, B. Wiedemann, Development of resistance in wild-type and hypermutable *Pseudomonas aeruginosa* strains exposed to clinical pharmacokinetic profiles of meropenem and ceftazidime simulated in vitro. *Antimicrob. Agents Chemother.* **51**, 3642–3649 (2007).

55. J. A. Good, C. Andersson, S. Hansen, J. Wall, K. S. Krishnan, A. Begum, C. Grundström, M. S. Niemiec, K. Vaitkevicius, E. Chorell, P. Wittung-Stafshede, U. H. Sauer, A. E. Sauer-Eriksson, F. Almqvist, J. Johansson, Attenuating *Listeria monocytogenes* virulence by targeting the regulatory protein PrfA. *Cell Chem Biol* **23**, 404–414 (2016).

56. H. Tükenmez, P. Singh, S. Sarkar, M. Çakır, A. H. Oliveira, C. Lindgren, K. Vaitkevicius, M. Bonde, A. E. Sauer-Eriksson, F. Almqvist, J. Johansson, A highly substituted ring-fused 2-pyridone compound targeting PrfA and the efflux regulator BrtA in *Listeria monocytogenes*. *MBio* **14**, e0044923 (2023).

57. B. Kreikemeyer, K. S. McIver, A. Podbielski, Virulence factor regulation and regulatory networks in *Streptococcus pyogenes* and their impact on pathogen-host interactions. *Trends Microbiol.* **11**, 224–232 (2003).

58. H. Persson, R. Vindebro, U. von Pawel-Rammingen, The streptococcal cysteine protease SpeB is not a natural immunoglobulin-cleaving enzyme. *Infect. Immun.* **81**, 2236–2241 (2013).

59. R. K. Carroll, J. M. Musser, From transcription to activation: How group A streptococcus, the flesh-eating pathogen, regulates SpeB cysteine protease production. *Mol. Microbiol.* **81**, 588–601 (2011).

60. G. C. Port, Z. T. Cusumano, P. R. Tumminello, M. G. Caparon, K. Federle, K. McIver, V. Panacholi, SpxA1 and SpxA2 Act coordinately to fine-tune stress responses and virulence in *Streptococcus pyogenes*. *MBio* **8**, e00288–e00217 (2017).

61. G. C. Port, E. Paluscio, M. G. Caparon, Complete genome sequence of emm Type 14 *Streptococcus pyogenes* strain HSC5. *Genome Announc.* **1**, e00612–e00613 (2013).

62. D. L. H. H. S. Courtney, D. L. Hasty, Aggregation of group A streptococci by human saliva and effect of saliva on streptococcal adherence to host cells. *Infect. Immun.* **59**, 1661–1666 (1991).

63. P. A. H. E. Hanski, P. A. Horwitz, M. G. Caparon, Expression of protein F, the fibronectin-binding protein of *Streptococcus pyogenes* JRS4, in heterologous streptococcal and enterococcal strains promotes their adherence to respiratory epithelial cells. *Infect. Immun.* **60**, 5119–5125 (1992).

64. M. Imohl, M. van der Linden, Antimicrobial susceptibility of invasive *Streptococcus pyogenes* isolates in Germany during 2003-2013. *PLOS ONE* **10**, e0137313 (2015).

65. CLSI Performance standards for antimicrobial susceptibility testing. 30th ed. CLSI Supplement M100. Wayne, PA: Clinical and Laboratory Standards Institute (2020).

66. W. Ni, X. Shao, X. Di, J. Cui, R. Wang, Y. Liu, In vitro synergy of polymyxins with other antibiotics for *Acinetobacter baumannii*: A systematic review and meta-analysis. *Int. J. Antimicrob. Agents* **45**, 8–18 (2015).

67. G. Orhan, A. Bayram, Y. Zer, I. Balci, Synergy tests by E test and checkerboard methods of antimicrobial combinations against *Brucella melitensis*. *J. Clin. Microbiol.* **43**, 140–143 (2005).

68. Z. Zou, R. F. Potter, W. H. McCoy IV, J. A. Wildenthal, G. L. Katumba, P. J. Mucha, G. Dantas, J. P. Henderson, *E. coli* catheter-associated urinary tract infections are associated with distinctive virulence and biofilm gene determinants. *JCI Insight* **8**, e161461 (2023).

69. A. L. Flores-Mireles, J. S. Pinkner, M. G. Caparon, S. J. Hultgren, EbpA vaccine antibodies block binding of *Enterococcus faecalis* to fibrinogen to prevent catheter-associated bladder infection in mice. *Sci. Transl. Med.* **6**, 254ra127 (2014).

70. J. Zahller, P. S. Stewart, Transmission electron microscopic study of antibiotic action on *Klebsiella pneumoniae* biofilm. *Antimicrob. Agents Chemother.* **46**, 2679–2683 (2002).

71. S. J. Hultgren, T. N. Porter, A. J. Schaeffer, J. L. Duncan, Role of type 1 pili and effects of phase variation on lower urinary tract infections produced by *Escherichia coli*. *Infect. Immun.* **50**, 370–377 (1985).

72. J. W. Rosch, F. F. Hsu, M. G. Caparon, Anionic lipids enriched at the ExPortal of *Streptococcus pyogenes*. *J. Bacteriol.* **189**, 801–806 (2007).

73. S. S. Justice, D. A. Hunstad, P. C. Seed, S. J. Hultgren, Filamentation by *Escherichia coli* subverts innate defenses during urinary tract infection. *Proc. Natl. Acad. Sci. U.S.A.* **103**, 19884–19889 (2006).

74. M. Kostakioti, M. Hadjifrangiskou, J. S. Pinkner, S. J. Hultgren, QseC-mediated dephosphorylation of QseB is required for expression of genes associated with virulence in uropathogenic *Escherichia coli*. *Mol. Microbiol.* **73**, 1020–1031 (2009).

75. T. K. Ulland, W. M. Song, S. C. Huang, J. D. Ulrich, A. Sergushichev, W. L. Beatty, A. A. Loboda, Y. Zhou, N. J. Cairns, A. Kambal, E. Loginicheva, S. Gilfillan, M. Cella, H. W. Virgin, E. R. Unanue, Y. Wang, M. N. Artyomov, D. M. Holtzman, M. Colonna, TREM2 maintains microglial metabolic fitness in Alzheimer's disease. *Cell* **170**, 649–663.e13 (2017).

76. P. S. Guiton, C. K. Cusumano, K. A. Kline, K. W. Dodson, Z. Han, J. W. Janetka, J. P. Henderson, M. G. Caparon, S. J. Hultgren, Combinatorial small-molecule therapy prevents uropathogenic *Escherichia coli* catheter-associated urinary tract infections in mice. *Antimicrob. Agents Chemother.* **56**, 4738–4745 (2012).

77. J. A. Merriman, W. Xu, M. G. Caparon, Central carbon flux controls growth/damage balance for *Streptococcus pyogenes*. *PLOS Pathog.* **19**, e1011481 (2023).

78. R. D. Regan, J. E. Fenyk-Melody, S. M. Tran, G. Chen, K. L. Stocking, Comparison of submental blood collection with the retroorbital and submandibular methods in mice (Mus musculus). *J. Am. Assoc. Lab. Anim. Sci.* **55**, 570–576 (2016).

79. T. J. Hannan, I. U. Mysorekar, C. S. Hung, M. L. Isaacson-Schmid, S. J. Hultgren, Early severe inflammatory responses to uropathogenic *E. coli* predispose to chronic and recurrent urinary tract infection. *PLOS Pathog.* **6**, e1001042 (2010).

80. L. Yu, V. P. O'Brien, J. Livny, D. Dorsey, N. Bandyopadhyay, M. Colonna, M. G. Caparon, E. D. Roberson, S. J. Hultgren, T. J. Hannan, Mucosal infection rewires TNFα signaling dynamics to skew susceptibility to recurrence. *eLife* **8**, e46677 (2019).

81. A. G.-F. W. J. Hopkins, A. Gendron-Fitzpatrick, E. Balish, D. T. Uehling, Time course and host responses to *Escherichia coli* urinary tract infection in genetically distinct mouse strains. *Infect. Immun.* **66**, 2798–2802 (1998).

82. G. G. Anderson, J. J. Palermo, J. D. Schilling, R. Roth, J. Heuser, S. J. Hultgren, Intracellular bacterial biofilm-like pods in urinary tract infections. *Science* **301**, 105–107 (2003).

83. A. Dobin, C. A. Davis, F. Schlesinger, J. Drenkow, C. Zaleski, S. Jha, P. Batut, M. Chaisson, T. R. Gingeras, STAR: Ultrafast universal RNA-seq aligner. *Bioinformatics* **29**, 15–21 (2013).

84. Y. Liao, G. K. Smyth, W. Shi, featureCounts: An efficient general purpose program for assigning sequence reads to genomic features. *Bioinformatics* **30**, 923–930 (2014).

85. R. Patro, G. Duggal, M. I. Love, R. A. Irizarry, C. Kingsford, Salmon provides fast and bias-aware quantification of transcript expression. *Nat. Methods* **14**, 417–419 (2017).

86. L. Wang, S. Wang, W. Li, RSeQC: Quality control of RNA-seq experiments. *Bioinformatics* **28**, 2184–2185 (2012).

87. M. D. Robinson, D. J. McCarthy, G. K. Smyth, edgeR: A Bioconductor package for differential expression analysis of digital gene expression data. *Bioinformatics* **26**, 139–140 (2010).

88. M. E. Ritchie, B. Phipson, D. Wu, Y. Hu, C. W. Law, W. Shi, G. K. Smyth, limma powers differential expression analyses for RNA-sequencing and microarray studies. *Nucleic Acids Res.* **43**, e47 (2015).

89. R. Liu, A. Z. Holik, S. Su, N. Jansz, K. Chen, H. S. Leong, M. E. Blewitt, M. L. Asselin-Labat, G. K. Smyth, M. E. Ritchie, Why weight? Modelling sample and observational level variability improves power in RNA-seq analyses. *Nucleic Acids Res.* **43**, e97 (2015).

90. P. Langfelder, S. Horvath, WGCNA: An R package for weighted correlation network analysis. *BMC Bioinformatics* **9**, 559 (2008).

91. M. W. Pfaffl, A new mathematical model for relative quantification in real-time RT-PCR. *Nucleic Acids Res.* **29**, 45e–445e (2001).

92. W. R. Lyon, C. M. Gibson, M. G. Caparon, A role for trigger factor and an rgg-like regulator in the transcription, secretion and processing of the cysteine proteinase of *Streptococcus pyogenes*. *EMBO J.* **17**, 6263–6275 (1998).

93. P. M. S. A. R. Hauser, P. M. Schlievert, Nucleotide sequence of the streptococcal pyrogenic exotoxin type B gene and relationship between the toxin and the streptococcal proteinase precursor. *J. Bacteriol.* **172**, 4536–4542 (1990).